Journal of
Applied
Crystallography
ISSN 0021-8898

Received 12 June 2010
Accepted 20 August 2010

Interesting growth features in potassium dihydrogen phosphate: unravelling the origin and dynamics of point defects in single crystals

G. Bhagavannarayana,[a]* P. Rajesh[b] and P. Ramasamy[b]

[a]Materials Characterization Division, National Physical Laboratory, Council of Scientific and Industrial Research, New Delhi 110012, India, and [b]SSN College of Engineering, SSN Nagar 603110, India. Correspondence e-mail: bhagavan@mail.nplindia.ernet.in

In a potassium dihydrogen phosphate single crystal grown by the temperature-lowering technique, some interesting growth features revealing the origin of point defects, their agglomeration and dynamics were observed. High-resolution X-ray diffractometry was employed for in-depth studies of the observed defects. Since the crucial properties of crystal-based devices are very much influenced by such defects, this is an important experimental finding with respect to improving growth techniques or conditions to avoid such defects.

1. Introduction

In recent years, organic, inorganic and semi-organic single crystals have been grown by a variety of techniques, such as the slow evaporation solution technique (SEST) (Vijayan *et al.*, 2006), the temperature-lowering technique (Shakir *et al.*, 2009), the recently invented solution-based Sankaranarayanan–Ramasamy (SR) method (Sankaranarayanan & Ramasamy, 2005), the well known Czochralski (CZ) method *etc*. These crystals have been characterized mostly by high-resolution X-ray diffractometry (HRXRD) and diffuse X-ray scattering (Bhagavannarayana, Ananthamurthy *et al.*, 2005) methods in order to evaluate their crystalline perfection. From these studies it is often observed that such crystals contain point defects and their aggregates, and in many cases they contain low-angle and very low angle structural grain boundaries (Bhagavannarayana, Ananthamurthy *et al.*, 2005). The possible reasons for these types of defects have also been pointed out (Vijayan *et al.*, 2006). However, because of their microscopic size, their origin in the crystal and their dynamic nature (in terms of movement and segregation) could not be demonstrated by any direct method. In the present investigation, we have been able to make such observations experimentally regarding point defects in a potassium dihydrogen phosphate (KDP) crystal grown by the temperature-lowering method with a high growth rate by fast reduction of temperature (0.4 K h^{-1}).

2. Experimental

2.1. Crystal growth

Pure KDP was grown from an aqueous solution with a simple apparatus that can be applied in certain forced convection configurations to maintain a high homogeneity of the solution. This apparatus consists of a seed rotation controller coupled with a stepper motor, which is controlled by using a microcontroller-based drive. This controller rotates the seed holder in the crystallizer in both directions (left and right). The seed crystal is mounted at the centre of a platform that is made of acrylic material and is fixed in the crystallizer. The seed mount platform stirs the solution very well and makes the solution more stable. Uniform rotation of the seed is required so as not to produce stagnant regions or recirculating flows, otherwise inclusions in the crystals will be formed owing to inhomogeneous supersaturation in the solution. The crystal growth was carried out in a 5000 ml standard crystallizer. The crystallizer temperature was controlled using an external water bath and the temperature fluctuations were less than 0.01 K. The saturation temperature was 317 K. The solution was filtered using Whatman filter paper of pore size 11 µm. After filtration, the solution was overheated to 328 K for 1 d. The temperature was then reduced by 3 K at 1 K h^{-1}, and subsequently the temperature was decreased to the saturation point at 1 K d^{-1}. A pure KDP crystal of size 10 × 10 × 8 mm was fixed at the centre of the crystallizer and kept inside a carefully controlled constant temperature bath. From the saturation point (317 K), the temperature was decreased at a rate of 0.02 K h^{-1} and, after 4 d of growth, the cooling rate was set at a rate of 0.04 K h^{-1} with a rotation of 35 r min^{-1}. After 20 d of growth, crystals with a size of approximately 30 × 30 × 45 mm were harvested (Fig. 1). Potassium dihydrogen phosphate was bought from M/S Merck (GR grade), Germany, and deionized water was obtained from the Millipore water purification unit. The resistivity of the deionized water is 18.2 MΩ cm.

2.2. High-resolution X-ray diffractometry

The crystalline perfection of the grown single crystals was characterized by HRXRD by employing a multicrystal X-ray diffractometer developed at the National Physical Laboratory, New Delhi (Lal & Bhagavannarayana, 1989). The well colli-

mated and monochromated Mo $K\alpha_1$ beam obtained from three monochromator Si crystals set in a dispersive (+,−,−) configuration was used as the exploring X-ray beam. The specimen crystal was aligned in the (+,−,−,+) configuration. Because of the dispersive configuration, though the lattice constants of the monochromator crystal(s) and the specimen are different, the unwanted dispersion broadening in the diffraction curve (DC) of the specimen crystal is insignificant. The specimen can be rotated about the vertical axis, which is perpendicular to the plane of diffraction, with a minimum angular interval of 0.4 arcseconds. The rocking or diffraction curves were recorded by changing the glancing angle (the angle between the incident X-ray beam and the surface of the specimen) around the Bragg diffraction peak position θ_B (taken as zero for the sake of convenience) starting from a suitable arbitrary glancing angle and ending at a glancing angle after the peak so that all the meaningful scattered intensities on both sides of the peak were included in the diffraction curve. The DC was recorded by the so-called ω scan wherein the detector is kept at the same angular position $2\theta_B$ with a wide opening for its slit. This arrangement is very appropriate for recording the short-range order scattering caused by defects or by the scattering from local Bragg diffractions from agglomerated point defects or from low-angle and very low angle structural grain boundaries (Bhagavannarayana & Kushwaha, 2010).

Before recording the DC, it was necessary to remove the non-crystallized solute atoms that remained on the surface of the crystal and any possible layers, which may sometimes form on the surfaces of crystals grown by solution methods (Bhagavannarayana *et al.*, 2006), and also to ensure the surface planarity. Therefore, the specimen was first lapped and then chemically etched in a non-preferential etchant of water and acetone mixture in a 1:2 volume ratio.

3. Results and discussion

As is very common, the KDP crystal was grown vertically along the *c* axis as shown in Fig. 1(*a*). In the figure, two clear-cut pyramid-shaped glittering regions resembling the top portion of the crystal can be seen well inside the crystal. As reported by Janssen-Van Rosmalen *et al.* (1978), this may be the consequence of a spongy capping zone on the (001) seed plate as KDP develops habit faces {100} (tetragonal prism) and {101} (tetragonal dipyramid), followed by clear further growth on the {101} pyramid faces. On top of the bottom pyramid, another pyramid also formed, which is, however, unexpected. The explanation given for the bottom pyramid by Janssen-Van Rosmalen *et al.* (1978) is not valid as the growth occurred on the {101} pyramid faces. Indeed, these pyramids were not observed during growth, only some cloudy structure, which was also observed in an L-asparagine monohydrate (LAM) crystal (Shakir *et al.*, 2010). In the present KDP specimen the cloudy structure later resolved as a clear pyramid(s). The most interesting observation is that, after a span of a month (after harvesting the crystal), a gas bubble was also found, visible at the tip of the bottom prism and indicated by an arrow in Fig. 1(*a*). On tilting the crystal, movement of the bubble was observed as a result of gravity, as seen in Figs. 1(*b*) and 1(*c*). In Fig. 1(*b*), the bubble has moved from the top to the right side as the crystal was bent left from the top. In Fig. 1(*c*) one can see that the bubble is trapped at a lower position in comparison with Fig. 1(*a*). This led us to the realization that the solvent occupies only a small volume situated near the tip of the pyramid defect structure. The formation of the bubble as a result of vacancy defects and its movement inside the crystal reveal the entrapment of solvent molecules and their dynamics, as described in the following.

Single crystals grown at any finite temperature cannot avoid vacancies and self-interstitials because of thermodynamical considerations (Wolf & Rauber, 1986). For example, in crystals grown by the CZ method, it is well known that a good number of vacancies (atoms or molecules missing from the assigned positions in the crystalline matrix) and self-interstitials (the atoms or molecules of the crystal dissolved in the interstitial space of the lattice) are expected to form at elevated temperatures during the growth process; their concentration decreases during the post-growth annealing by the process of out-diffusion of these defects, including various impurities that may have been present in the initial charge and/or originated from the crucibles. However, the process of out-diffusion of point defects is very slow and the time duration of a few days or tens of hours is not enough for complete out-diffusion of defects. During the cooling process these defects also try to segregate in different shapes and sizes as the free energy of the total system is less when they are in the clustered form. This clustering may lead to the formation of structural grain boundaries as the strain generated by such clustered defects is high enough and the strain releases through such processes. The formation of very low angle and low-angle structural boundaries was clearly observed in bismuth germanium oxide (Choubey *et al.*, 2002) and lithium niobate (Bhagavannarayana, Budakoti *et al.*, 2005) crystals

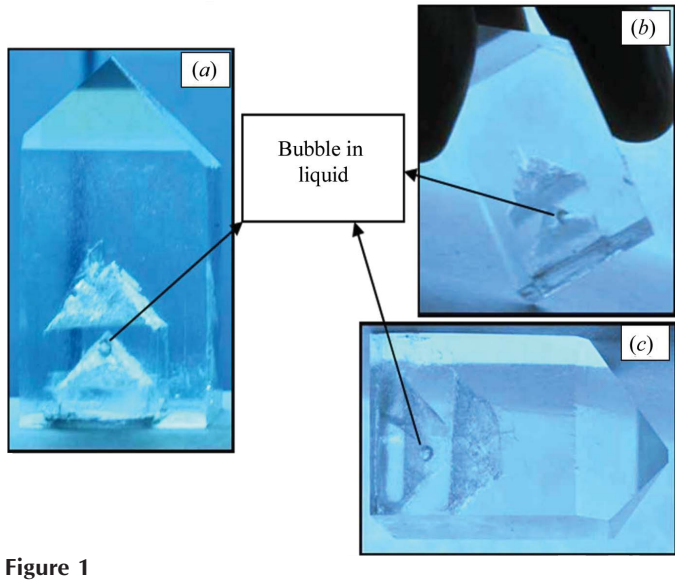

Figure 1
A bubble inside a KDP single crystal in aqueous medium, moving as a result of gravity with changes in its orientation.

grown by the CZ method; with a prolonged annealing process, such boundaries were also found to be annealed out. These types of boundaries were also observed in SEST-grown crystals. In this method, the crystal grows at a constant temperature. However, the atoms/molecules that are taking part in the growth at the solid–liquid interface are always subjected to bombardment by the atoms in the liquid, because of kinetic energy at all finite temperatures. This leads to the formation of vacancies and self-interstitials and the entrapment of solvent molecules as defects inside the crystal. Two good examples are benzimidazole (Vijayan *et al.*, 2006) and LAM (Shakir *et al.*, 2010) single crystals. In the LAM crystal, a cloud of point defects or clusters of defects could be seen with the naked eye in the central part of the crystal. These defects are responsible for the observed very low angle boundaries, along which they are segregated. Low-temperature annealing leads to a reduction of such defects and thus significant improvement in device properties (Shakir *et al.*, 2010; Bhagavannarayana, Choubey *et al.*, 2005).

As illustrated above, during the growth process, along with the formation of vacancy and interstitial defects due to the fast growth rate in the present KDP crystal, one would expect a good number of solvent (water) molecules to become entrapped inside the crystal. These entrapped solvent molecules in the course of time try to move out of the crystal by the process of out-diffusion, as a result of the self-created stress, and in this process the molecules near the surface seem to succeed. However, the solvent molecules, vacancies and self-interstitials that try to move towards the central regions agglomerate initially into small clusters, seen as a cloud inside the crystal as the crystal is fully transparent to visible light, as in the case of LAM (Shakir *et al.*, 2010). Depending upon the density, the clustered vacancies appear as voids. The tensile stress developed by the voids could be responsible for further agglomeration of defects. After massive agglomeration of vacancies a good volume of vacant space has been created and some part of it is filled with entrapped water molecules. The vacant space may be converted into water vapour as a result of the presence of entrapped water and behaves as a gas bubble. The entrapped water could dissolve some of the KDP and hence the observed liquid might be a saturated KDP solution. That is how one could regard the moving bubble inside the liquid. However, if the concentrations of entrapped solvent molecules and vacancies are not high enough, they may remain as isolated defects or small-sized agglomerates and hence they may not form into a supersaturated solution and gas bubble inside the crystal. It is worth mentioning here that, during thermal annealing, defect dynamics were observed through X-ray topography (Bhagavannarayana, Choubey *et al.*, 2005), but in the present investigation they were observed even at room temperature (during and after growth).

To reveal more details about the crystalline perfection, high-resolution X-ray diffraction or rocking curves (RCs) were recorded by employing an in-house-developed high-resolution multicrystal X-ray diffractometer (Lal & Bhagavannarayana, 1989). RCs were recorded under identical experimental conditions at four positions (1, 2, 3 and 4) of the specimen crystal as shown in the left-hand-side inset of Fig. 2(*a*). It may be mentioned here that the RC contains information mostly from the near-surface regions of the crystal, but these surface regions could be influenced by the state of the inner regions as revealed in the following. Figs. 2(*a*) and 2(*b*) depict the RCs recorded at positions 1 and 2, respectively, which are far from the defect pyramids; both curves have a single peak with the same full width at half-maximum (FWHM) of 9.5 arcseconds, revealing the fact that these regions have good crystalline perfection and are free from structural grain boundaries (Bhagavannarayana, Choubey *et al.*, 2005) and mosaic spread (Bhagavannarayana & Kushwaha, 2010). For a crystal with structural grain boundaries, the rocking curve contains more than one peak corresponding to different crystal blocks (or grains) which are misoriented with respect to each other (*e.g.* Fig. 1 of Bhagavannarayana, Ananthamurthy *et al.*, 2005). When the crystal contains mosaic spreads (small crystallites of sub-μm- or nm-

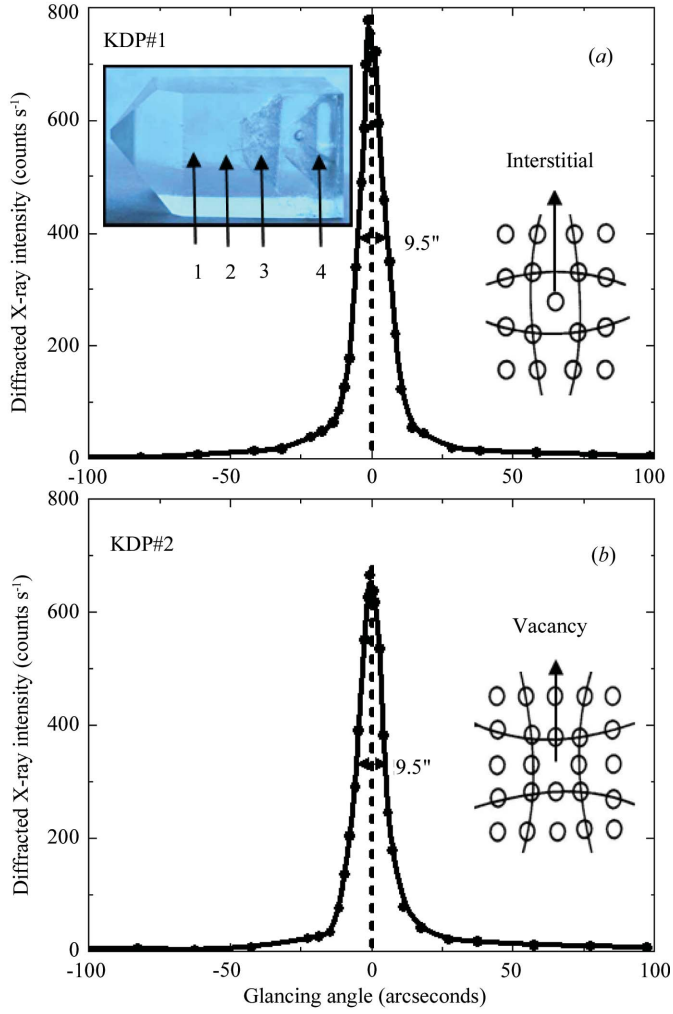

Figure 2
RCs recorded for a KDP crystal using (200) diffracting planes: (*a*) and (*b*) are, respectively, for regions 1 and 2 as indicated in the inset on the left-hand side. The insets on the right-hand sides of (*a*) and (*b*), respectively, depict schematically how the interstitial and vacancy defects influence the lattice spacing around the defect core.

sized spread in the main crystal block which are misoriented with respect to each other), the rocking curve cannot be a sharp peak with good peak intensity. It will be rather broad and its FWHM value may be in arcminutes or even degrees but not of the order of a few arcseconds. A good example of such a curve is the very broad peak with an angular spread of around 300 arcseconds (5 arcminutes) of Fig. 6(*c*) of Bhagavannarayana & Kushwaha (2010). The rocking curves of the present sample do not contain such features. However, on careful observation, one can see asymmetry in the RCs of regions 1 and 2. For a particular angular deviation ($\Delta\theta$) of glancing angle with respect to the peak position, the scattered intensity is slightly higher in the positive direction than in the negative direction. This feature clearly indicates that regions 1 and 2 of the crystal contain predominantly the interstitial type of defects rather than vacancy defects. This can be understood by the fact that, in the presence of interstitial defects (self-interstitials or impurities or dopants at interstitial sites), the lattice around these defects undergoes compressive stress (Bhagavannarayana *et al.*, 2008). This situation is shown schematically in the right-hand inset of Fig. 2(*a*). Hence the lattice parameter d (interplanar spacing) decreases, which leads to more scattered (also known as diffuse X-ray scattering) intensity at higher angles (positive side of the peak) along the wings or tails of the RC with respect to the exact Bragg peak position θ_B (which is taken as zero here) as d and $\sin\theta_B$ are inversely proportional to each other in the Bragg equation ($2d\sin\theta_B = n\lambda$; n and λ being the order of reflection and wavelength, respectively, which are fixed). As the stress due to point defects and their aggregates is very localized, the variation in d spacing is very local and the scattering is of short-range order. The actual d values (or the lattice parameters) and the corresponding Bragg angles of the overall crystal do not change. The converse explanation is true in the case of vacancy defects, which cause tensile stress in the lattice around the defect core, leading to an increase of lattice spacing (right-hand inset of Fig. 2*b*), which in turn results in more scattered intensity at lower angles (*i.e.* negative side of the peak) with respect to the exact Bragg peak position θ_B. However, one cannot rule out the absence of vacancy defects in regions 1 and 2, as the scattered intensity at lower angles (Figs. 2*a* and 2*b*) is significantly higher than that observed in an RC (with FWHM 2.7 arcseconds) obtained for a nearly perfect KDP crystal (Dhanaraj *et al.*, 2008) recorded under identical conditions with the same diffractometer (Lal & Bhagavannarayana, 1989).

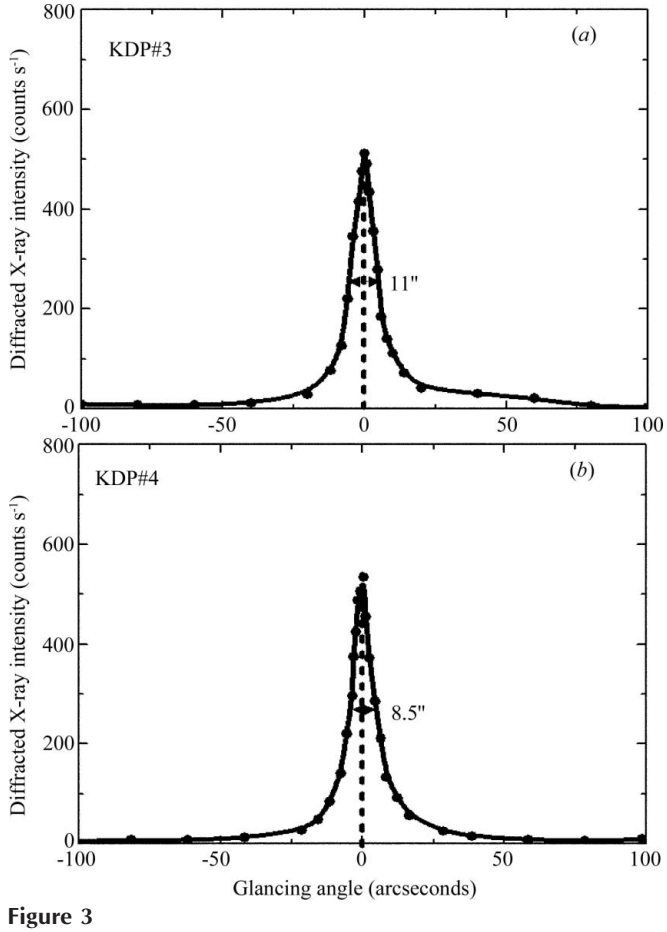

Figure 3
RCs recorded for a KDP crystal using (200) diffracting planes: (*a*) and (*b*) are, respectively, for regions 3 and 4 as indicated in the inset of Fig. 2.

Figs. 3(*a*) and 3(*b*) show the RCs, respectively, for regions 3 and 4, with FWHM values of 11 and 8.5 arcseconds. The fact that region 4 exhibits the lowest value of FWHM (8.5 arcseconds; Fig. 3*b*) indicates that this region within the spongy pyramid contains liquid, and the gas bubble possesses the least number of point defects. It is thus revealed that vacancies and interstitial water molecules have been removed from this region by the process of guttering (Bhagavannarayana & Kushwaha, 2010) into the spongy pyramid, which is in tune with the visual observation (Fig. 1). However, the RC of region 3 (Fig. 3*a*), with the highest FWHM value, indicates that this region, where no guttering could be seen, contains predominantly the interstitial type of point defects and their aggregates due to entrapped solvent molecules. The intermediate value of 9.5 arcseconds for regions 1 and 2 indicates that the incorporation of vacancies and solvent molecules is much less in these regions, which might be because the growth rate in these regions became slower as the concentration of the supersaturated solution was reduced by the time the crystal reached these regions.

4. Conclusions

Certain interesting growth features of point defects, which commonly occur in single crystals but are difficult to observe directly, such as their origin, clustering and dynamics, have been demonstrated in a potassium dihydrogen phosphate crystal grown at an intentionally fast growth rate by the temperature-lowering method. The details of these features are well explained through HRXRD. The present investigation also sheds light on the fact that the origin of most crystal defects is point defects. These are dynamic in nature and transform into a variety of macroscopic defects through clustering and propagation by self-generated strains so as to come to the lowest possible free energy state. Thereby the most stable state of the crystal is attained.

References

Bhagavannarayana, G., Ananthamurthy, R. V., Budakoti, G. C., Kumar, B. & Bartwal, K. S. (2005). *J. Appl. Cryst.* **38**, 768–771.

Bhagavannarayana, G., Budakoti, G. C., Maurya, K. K. & Kumar, B. (2005). *J. Cryst. Growth*, **282**, 394–401.

Bhagavannarayana, G., Choubey, A., Shubin, Yu. V. & Lal, K. (2005). *J. Appl. Cryst.* **38**, 448–454.

Bhagavannarayana, G. & Kushwaha, S. K. (2010). *J. Appl. Cryst.* **43**, 154–162.

Bhagavannarayana, G., Parthiban, S. & Meenakshisundaram, S. (2006). *J. Appl. Cryst.* **39**, 784–790.

Bhagavannarayana, G., Parthiban, S. & Meenakshisundaram, S. (2008). *Cryst. Growth Des.* **8**, 446–451.

Choubey, A., Bhagavannarayana, G., Shubin, Yu. V., Chakraborty, B. R. & Lal, K. (2002). *Z. Kristallogr.* **217**, 515–521.

Dhanaraj, P. V., Mahadevan, C. K., Bhagavannarayana, G., Ramasamy, P. & Rajesh, N. P. (2008). *J. Cryst. Growth*, **310**, 5341–5346.

Janssen-Van Rosmalen, R., Van der Linden, W. H., Dobinga, E. & Visser, D. (1978). *Krist. Technol.* **13**, 17–28.

Lal, K. & Bhagavannarayana, G. (1989). *J. Appl. Cryst.* **22**, 209–215.

Sankaranarayanan, K. & Ramasamy, P. (2005). *J. Cryst. Growth*, **280**, 467–473.

Shakir, M., Kushawaha, S. K., Maurya, K. K., Kumar, S., Wahab, M. A. & Bhagavannarayana, G. (2010). *J. Appl. Cryst.* **43**, 491–497.

Shakir, M., Kushwaha, S. K., Maurya, K. K., Arora, M. & Bhagavannarayana, G. (2009). *J. Cryst. Growth*, **311**, 3871–3875.

Vijayan, N., Bhagavannarayana, G., Kanagasekaran, T., Ramesh Babu, R., Gopalakrishnan, R. & Ramasamy, P. (2006). *Cryst. Res. Technol.* **41**, 784–789.

Wolf, S. & Rauber, R. N. (1986). *Silicon Processing for the VLSI Era*, Vol. 1, *Process Technology*. Sunset Beach: Lattice Press.